Kumnorkaew, Theerawat; Lian, Junhe; Uthaisangsuk, Vitoon; Bleck, Wolfgang

Effect of ausforming on microstructure and hardness characteristics of bainitic steel

Published in:
Journal of Materials Research and Technology

DOI:
10.1016/j.jmrt.2020.09.016

Published: 01/11/2020

Document Version
Publisher's PDF, also known as Version of record

Available online at www.sciencedirect.com

jmr&t Journal of Materials Research and Technology

https://www.journals.elsevier.com/journal-of-materials-research-and-technology

Original Article

Effect of ausforming on microstructure and hardness characteristics of bainitic steel

Theerawat Kumnorkaew[a,*], *Junhe Lian*[b,*], *Vitoon Uthaisangsuk*[c], *Wolfgang Bleck*[a]

[a] *Steel Institute of RWTH Aachen University, 52072 Aachen, Germany*

[b] *Advanced Manufacturing and Materials, Department of Mechanical Engineering, Aalto University, Puumiehenkuja 3, 02150 Espoo, Finland*

[c] *Department of Mechanical Engineering, King Mongkut's University of Technology Thonburi, 10140 Bangkok, Thailand*

ARTICLE INFO

Article history:
Received 2 July 2020
Accepted 2 September 2020

Keywords:
Ausforming
Low-carbon CFB steel
M/A constituent
Grain refinement
Deformation temperature
Strain rate

ABSTRACT

Effects of process parameters of the ausforming such as temperature, strain and strain rate on the martensitic start temperature, kinetics of isothermal bainitic transformation and microstructure refinement of a low carbon carbide-free bainitic steel were investigated. It was found that applying plastic deformation to untransformed austenite during intermediate temperatures decreased the martensite start temperature of steel and enabled isothermal bainitic transformation at low temperatures. Hereby, ausforming significantly generated heterogeneous nucleation sites, which accelerated the overall kinetics of bainitic transformation and thus increased bainitic phase fraction in steel. In addition, the ausforming enhanced the stability of austenite that led to reduced amount of martensite after cooling down to room temperature. Finally, the ausforming parameters and observed microstructure features were correlated and discussed along with the hardness of steel.

1. Introduction

The requirement of high-performance steels with lower production cost and better machinability has led to development of carbide free bainitic (CFB) steel. This CFB steel mainly consisted of fine lath matrix of bainitic ferrite (BF) embedded with retained austenite (RA). This RA was certainly a residual product from the process of carbon partitioning between supersaturated bainitic ferrite and surrounding austenite during a bainitic transformation. Such partitioning resulted in a formation of film-like or blocky RA that exhibited different stabilities [1]. The strengthening mechanism of CFB steel was mostly controlled by the contribution of BF, whereas its toughness and ductility are governed by the volume fraction and shape of RA [2,3]. According to Caballero and Mateo [4], RA could affect the strengthening mechanism of steel by the transformation-induced plasticity (TRIP) effect. It was obviously shown that controlling the stability of RA played an important role in balancing mechanical properties (ductility, strength, and toughness) regarding the TRIP effect, which strongly depended on its chemical composition and morphological feature.

As reported in [5,6] a film-like RA was a slender phase and located between BF sheaves. The film-like RA was more stable and difficult to be transformed to untempered martensite

* *Corresponding authors.*
E-mails: theerawat.kumnorkaew@iehk.rwth-aachen.de (T. Kumnorkaew), junhe.lian@aalto.fi (J. Lian).

https://doi.org/10.1016/j.jmrt.2020.09.016

during either final quenching or deformation at a lower temperature in comparison to the blocky type RA due to its higher degree of carbon enrichment. The blocky RA was usually found in the form of an inequiaxed blocky shape and dispersed among the granular matrix of BF, in which its stability directly depended on the block size. Liu et al. [5] showed that large blocky RA was unstable and could partially transformed into high-carbon brittle martensite during cooling down to room temperature, while smaller RA blocks were more stable. However, blocky RA exhibited lower stability than the film-like RA. Such unstable feature was often called 'M/A' phase, because it basically contained both martensite and untransformed RA. This untransformed RA could be completely transformed into a fully martensitic structure during an early stage of deformation [6–8]. Although the existence of brittle martensite was beneficial to hardness and strength in general, it was a major factor for deteriorating ductility and impact toughness of steels, since it could lead to a severe localization of neighboring phases due to the large difference in terms of strength [9].

Numerous works have been conducted in the past decades, in which the M/A constituents were replaced with fine and stable structures by different methods [5,10,11]. It was suggested that increasing the volume fraction of bainite and the possibility of austenite decomposition could be solutions of this critical issue [12]. Principally, the bainitic transformation started by para-equilibrium nucleation and grew through shear mechanism induced by diffusionless transformation [13]. Nevertheless, the transformation will be completely terminated when carbon was partitioned into austenite immediately after the bainitic growth approached the T_0' locus of equilibrium phase diagram, in which the strain energy of BF was taken into account [7,14,15]. It is also known that carbon is the main element which governed the phase transformation in steel. Increasing of carbon concentration enhanced the thermal stability of austenite and subsequently decreased the transformation temperature. Bhadeshia [16] reported that microstructure refinement of low-alloy bainitic steels was achieved well at very low transformation temperatures for steel containing 0.3–1.0%C. On the other hand, the phase transformation in those high/medium-carbon steels was time-consuming, possibly taking several days to complete the process [3].

Moreover, there have been attempts to apply the concept of lowering transformation temperature to low-carbon CFB steels (%C $\leq$ 0.2%) because of their better weldability and wear resistance, accompanied by other high-performance features [11,17]. Indeed, the typical heat treatment used for producing such ultrafine-grained bainitic steel by isothermal tempering above the martensite start (Ms) temperature was by far unpractical, because insufficient enrichment of carbon in austenite caused an inability of lowering transformation temperature. Subsequently, it led to a low thermal stability of austenite and allowed the formation of M/A constituent [18,19]. Hence, ausforming as a thermomechanical heat treating process can be applied in order to overcoming the limitation by means of applying external load to the untransformed austenite. The advantage of this process is to increase the thermal stability of austenite by introducing structural defects and thus to enable the bainitic transformation at a lower temperature. It also generated sub-grain boundaries, which led to a refinement of prior austenitic grain structure [20,21]. These defects could further facilitate additional nucleation sites for subsequent bainitic transformation, in which its transformation kinetics was accelerated. In contrast, occurred nuclei could then transformed to smaller amount of bainite due to mechanical stabilization of the austenite. Such mutual effects were clearly verified by experimental studies concerning ausforming heat treatment of medium/high carbon steels [22–28]. However, a few studies have been done for low-carbon steels [29,30]. The transformation kinetics of bainite and systematic correlation between ausforming parameters, microstructure evolution and mechanical properties of low-carbon steels remain unclear.

Therefore, in this work influences of processing parameters of ausforming including deformation temperature, strain and strain rate on the isothermal bainitic transformation behaviour, microstructure refinement and hardness of a low-carbon CFB steel were investigated by means of thermo-mechanical simulation. Each single control variables were systematically studied. Except for the ausforming parameters, other thermal histories of the examined samples was kept the same in the dilatometry tests of all cases. The microstructures of thermo-mechanically treated samples were characterized by light optical microscopy (LOM) and scanning electron microscopy (SEM). Afterwards, volume fraction of M/A and bainite including their morphologies were analyzed. In addition, X-ray diffraction (XRD) was employed to quantify the volume fraction of RA. It should be noted that the main focus of the current study was effects of processing parameters on emerged microstructure development. Therefore, resulting mechanical properties have been not elaborated and size of used samples in the thermal-mechanical treatment was also limited. The strength property was investigated by using a hardness measurement. Detailed discussions on the correlation of processing parameters with determined microstructure features and hardness values were provided.

2. Materials and methods

2.1. *Materials*

A low-carbon CFB steel containing 0.18%C, 0.97%Si, 2.5%Mn, 0.002%B, and 0.033Ti by weight was investigated in this work. The amounts of Si and Mn in the examined steel were verified to be adequate for a development of CFB steel [31]. Hereby, the addition of Mn aimed to increase the stability of RA and hardenability of steel, whereas Si could suppress the formation of cementite in bainitic structure and facilitate an enrichment of carbon in austenite during the bainitic transformation. Moreover, adding such a little amount of Ti could also prevent the formation of boron nitride at the ferrite/austenite interfaces by forming either titanium nitride (TiN) or titanium carbonitride (Ti(C, N)) with nitrogen. The test material was initially produced in a laboratory vacuum induction furnace and cast into an 80 kg block with a cross-section of 140 $\times$ 140 mm^2. Subsequently, the ingot was homogenized at 1250 °C for 2 h and pre-forged into a final cross-section of 60 $\times$ 60 mm^2 by the

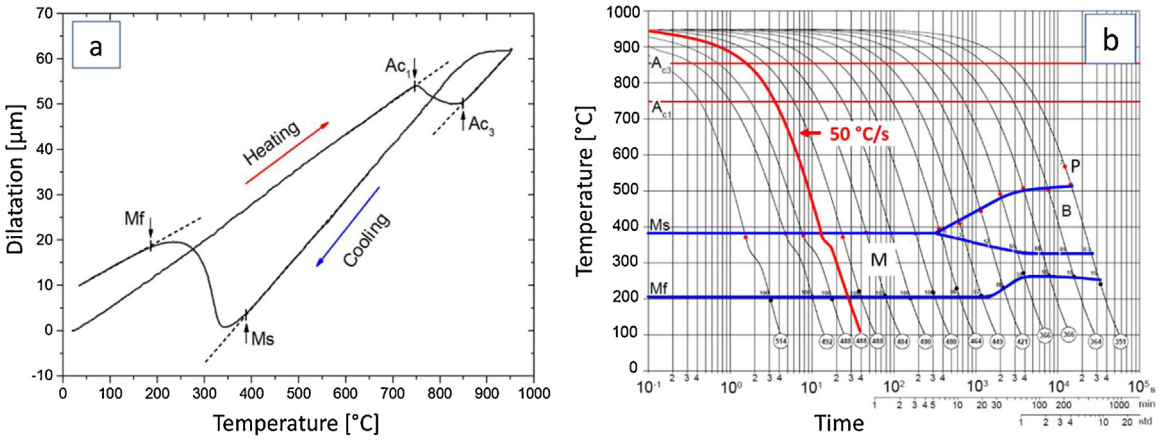

Fig. 1 – (a) Radial dilatation vs. temperature during heating and cooling and (b) experimental CCT diagram of the investigated steel (M, B, and P stand for martensitic, bainitic, and pearlite transformation regimes, respectively).

semi-product simulation center (SPSC) prior to cooling down to room temperature (RT).

2.2. *Dilatometry*

To investigate the influences of processing parameters of ausforming on the kinetics of phase transformation, microstructure evolutions and hardness of steel, cylindrical specimens with a diameter of 5 mm and length of 10 mm were machined from the homogenized billet along the direction perpendicular to the forging direction. The thermomechanical experiments were carried out using a Bähr DIL805 dilatometer. Before each test, a Pt/Pt/-10 Rh thermocouple (type S) was spot-welded on the surface of central area of specimens for measuring temperature development. The specimens were then placed between two quartz rods and in the middle of an induction coil. A cooling system with helium gas and laser infrared detector for determining displacement of specimen in the radial direction were installed. Note that such measured radial displacement could be also used to gather a volumetric change of specimen. An example of radial dilatation vs. temperature diagram, which was recorded throughout the heating and cooling stages in the dilatometry test is illustrated in Fig. 1**a**. By a heating rate of 18 °C/s from RT to the austenitizing temperature of steel at 950 °C, the observed first inflection point represented the Ac1 temperature of 745 °C and finish temperature Ac3 of 855 °C for the austenitic transformation. When cooling down at a rate of 50 °C/s, the first deviation of tangent line around 390 °C was the martensite start (Ms) temperature and the temperature of about 172 °C was the martensite finish (Mf) temperature. Fig. 1**b** exhibits the continuous cooling transformation (CCT) diagram of the investigated steel, which was determined from dilatometry tests at various cooling rates after austenitizing at 950 °C for five minutes. It was found that a fully martensitic structure likely formed when a cooling rate higher than ~1.5 °C/s was employed.

In this study, four different heat-treatment routes (I to IV) were applied, as presented in Fig. 2. The routes I and III were designed to investigate the effect of ausforming on the Ms temperature. The decomposition behaviour of austenite to bainite affected by ausforming was studied by the routes II and IV or so-called pure isothermal tempering (PIT). Note that the tempering stage defined at 400 °C was aimed to experimentally verify the martensitic transformation. The results obtained from specimens passed through routes I and II were considered as a reference for comparison with those from routes with ausforming. For specimens subjected to ausforming, Ms temperature was also identified. In the case of ausforming route III, deformation temperature was varied between 650 °C and 800 °C, while final strain and strain rate of 0.78 and 1 s^{-1} were employed, respectively. For the ausforming route IV, all temperatures, final strains and strain rates, as given in Table 1, were taken into account. At the beginning of the heat treatments, all specimens were heated to the austenitizing temperature of 950 °C with the rate of 18 °C/s and held for 300 s for achieving a homogeneous microstructure. The cooling rate to the tempering temperature of 50 °C/s was set for both specimens with and without ausforming. For the PIT treatment, specimens were soaked at the temperature of 400 °C for 1 h and further cooled down to RT at the rate of 20 °C/s. It is noted that prior to deformation by ausforming, specimens were held for 10 s so that thermal gradient caused by the fast cooling could be first eliminated. The similar concept was also applied in [30]. During the cooling stages of each routes, radial dilatations of specimens were gathered in order to examine the phase transformation characteristics. To evaluate the kinetics of the isothermal bainitic phase transformation under different conditions, the dilatation data obtained at 400 °C was additionally determined and afterwards normalized using the formula: $(d_i–d_0)/d_0$, where d_i and d_0 represent the instantaneous diameter during tempering and diameter after deformation before the isothermal holding, respectively [25].

2.3. *Microstructure analysis and hardness test*

Microstructure analyses and hardness measurements were performed at the center of cross-sectional area of thermomechanically treated specimens parallel to the compression

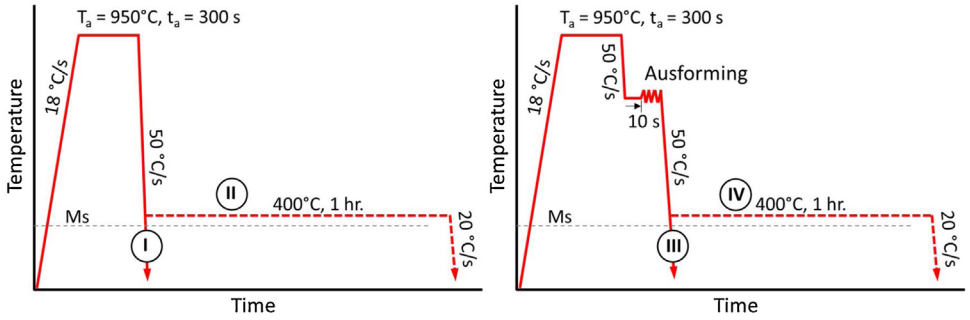

Fig. 2 – Thermomechanical treatment routes through direct quenching (I, III) and tempering (II, IV) with and without ausforming.

Table 1 – Variations of temperature, strain and strain rate applied in the ausforming routes III and IV.

Parameters Type of investigation	Temperature (°C)	Strain rate (s^{-1})	Strain (–)
Effect of deformation strain	650	1	0.15, 0.78
Effect of deformation temperature	650, 700, 750, 800	1	0.78
Effect of deformation strain rate	650	0.1, 1, 10	0.78

direction. The microstructures were examined by both light optical microscope (LOM) and scanning electron microscope (SEM). The quantitative identifications of observed phases were done by using X-ray diffraction (XRD) on BRUKER D8 diffractometer. All specimens for LOM and SEM were mechanically ground with abrasive papers (no. 600, 1200, and 2400) and then further polished with fine diamond paste. Different types of etching procedures were applied for metallographic specimens. For observing prior austenitic grains, specimens were etched with saturated picric acid and distilled water, heated at 60 °C for 30 s in a water bath, while for microstructure examination they were etched with Klemm's solution. In case of SEM investigations, etching with a 3% Nital solution was used. On the other hand, specimens prepared for XRD measurement were electro-polished by a TenuPol-5 single-jet electro-polishing device. Hereby, A2 electrolyte was employed at room temperature with the voltage and flow rate at 40 V and 12 mm/s, respectively. The XRD machine was set by using a filtered CuK_α radiator, which was operated at 40 kV and 30 mA under the collection range between 30° and 120° at a step width of 0.01° with counting time of 2 s. The phase fractions of face-centered cubic (FCC) RA and body-centered cubic (BCC) bainitic ferrite or/and martensite were subsequently analyzed by the Rietveld's refinement method using MAUD software. Macro-Vickers hardness measurements were conducted, in which a constant load of 10 kg and holding time of 15 s according to the ASTM E92-17 standard were applied.

3. Results and discussions

3.1. *Martensite start temperature and prior austenite grain*

First, effects of ausforming and deformation temperature on the radial dilatation during martensitic transformation and prior austenitic grains of directly quenched specimens after austenitizing/ausforming heat-treatments are displayed in Fig. 3. It was found in Fig. 3a that lowering deformation temperature of ausforming resulted in shifting of the Ms temperature. It decreased from the temperature of around 382 °C to 363 °C when the ausforming temperature was reduced from 800 °C to 650 °C. This could be due to the fact that during the hot deformation crystal defects and grain boundaries were increased, while prior austenitic grain (PAG) size was reduced. As a consequence, the strength of undercooled austenite increased before the transformation of martensite. Particularly, at lower temperatures, where effect of work hardening on the generation of substantial crystal defects was pronounced, the contribution to austenite strengthening was thus more significant. Generally, the strength of prior austenite played a major role in the subsequent phase transformation with regard to mechanical stabilization. Hereby, the austenite to martensite transformation of steel was resisted so that its Ms temperature was lowered and an isothermal bainitic transformation was enabled at low temperature [22,32]. Additionally, it is noted that during the martensitic transformation another small slope change was observed nearby the Mf temperature. Such uneven transition occurred only in the deformed specimens and its degree depended on the ausforming temperature. This phenomenon was also reported for some steels, especially highly alloyed chromium steels in [33,34]. It was evidenced that carbide precipitation and/or growth of existing carbides could lead to an inhomogeneous distribution of alloying element in austenite, which resulted in a discontinuous characteristic of austenite to martensite transformation between the Ms and Mf temperature. However, in this work, the soaking time of 300 s at the austenitization temperature of 950 °C was applied, which was sufficient for achieving a complete solid solution of austenite without remaining carbides in the steel. Note that this slope change was not observed in the specimens without ausforming and the discontinuity was more pronounced when the deformation temperature became higher. Therefore, such discontinuous transformation was likely caused by ausforming accelerated/induced carbide precipitation. It seemed that larger difference between ausforming and Ms temperature led

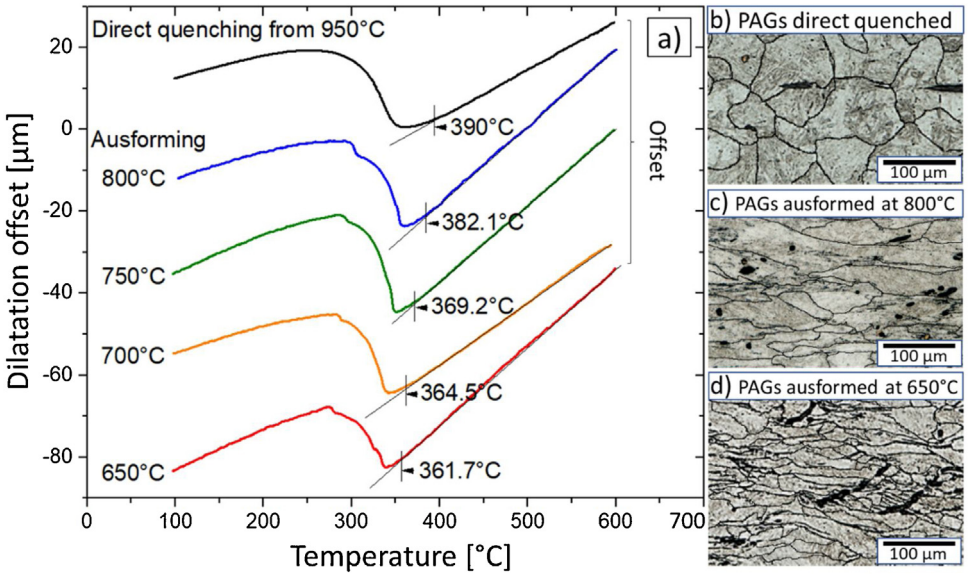

Fig. 3 – (a) Ms temperatures determined by the dilations and (b)–(d) prior austenitic grains of specimens after direct quenching from austenitization temperature (route I) and those quenched after ausforming at various temperatures (route III).

to more noticeable slope change. Additional investigations are needed to verify this occurrence. Moreover, the PAGs of ausformed specimens were horizontally elongated, in which its magnitude directly depended on the deformation temperature. It was found that ausforming caused pancaking of prior austenite grains and it became more severe at lower ausforming temperature, for instance, at 650 °C, as depicted in Fig. 3**b–d**. It was due to the increase of boundary areas of prior austenite per unit volume/area.

3.2. *Dilatation characteristic during phase transformation*

Fig. 4 shows the radial dilatation vs. temperature curves of specimens during the cooling stages of applied thermomechanical treatment (routes II and IV). From the beginning of austenitization temperatures or from the ausforming temperature to the tempering temperature at 400 °C, all dilatation curves exhibited almost linear behaviour which showed no phase transformation occurred. Then, by decomposition of austenite to bainitic ferrite the curves rose up vertically until the transformation completed. Hereby, amount of transformed bainite could be approximately estimated by measuring such a vertical change [35]. In the final stage from the temperature of 400 °C to room temperature, all curves deviated from the given tangential (dashed) lines. These dashed lines were drawn individually on each experimental curve by a linear regression with respect to the deformation conditions. These obvious deviations were caused by decomposition of residual austenite into harder martensite. Larger deviation implied increased amount of transformed martensite. In Fig. 4a, the vertical arrows showed the estimated temperatures at the onset of the transformation. The martensitic transformation of specimen after PIT took place at the temperature of 351 °C, whereas those of specimens deformed at 650 °C/1s^{-1} until the strain of 0.15 and 0.78 were around 270 °C and 183 °C, respectively. The dilatation characteristics exhibited that lower fraction of martensite was transformed in ausformed specimens in comparison with that in PIT specimen. In addition, variation of the ausforming temperature also significantly affected the deviation of curves, as shown in Fig. 4**b**. The decomposition of residual austenite to martensite tended to be increased when the ausforming temperature became higher. The results were in consistent with those reported in [22,32]. However, effect of varying strain rate of the ausforming on the martensitic transformation was negligible, as seen in Fig. 4**c**. The martensitic fractions in the specimens subjected to different strain rates were not much differed, especially when ausforming between the strain rate of 0.1 s^{-1} and 1 s^{-1}.

3.3. *Kinetics of bainitic transformation*

The decomposition of deformed austenite into bainite could be identified by the relative dilation at the isothermal tempering stage, since there was no other phase transformation occurred [36]. Hereby, the dilatation rate was interpreted as the rate of phase transformation. Fig. 5**a** illustrates the kinetics of bainitic transformation of specimens deformed at the temperature of 650 °C, strain rate of 1 s^{-1} until the final strains of 0.15 and 0.78 in comparison with that of PIT samples. It was found that the bainitic transformation behaviour of steel could be considerably altered by applying ausforming. Both onset and completion of the transformation were accelerated when ausforming strain was increased. The magnitude of transformation in the PIT specimen was rather low. The ausforming caused crystal defects within former austenitic grains during deformation e.g. deformation bands, sub-grain boundaries and dislocation [37]. These generated defects further enhanced nucleation sites for the bainitic

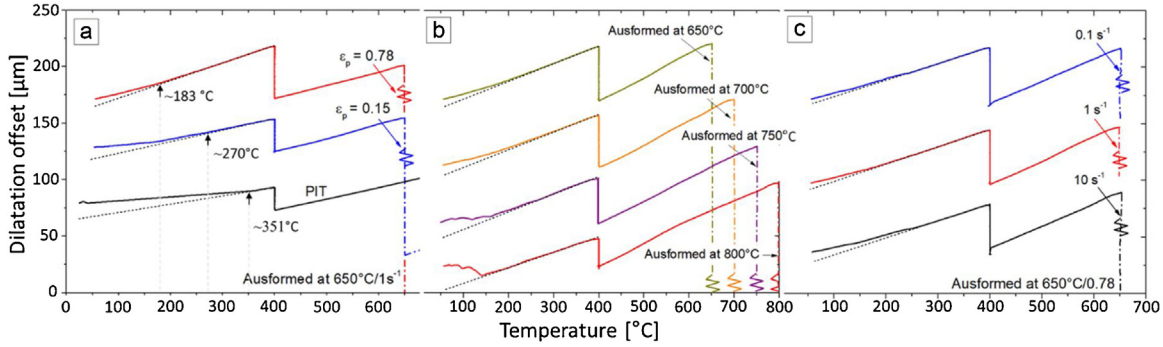

Fig. 4 – Radial dilatation vs. temperature curves from the entire cooling stage after ausforming at various (a) strains (b) temperatures and (c) strain rates of specimens from route II and IV.

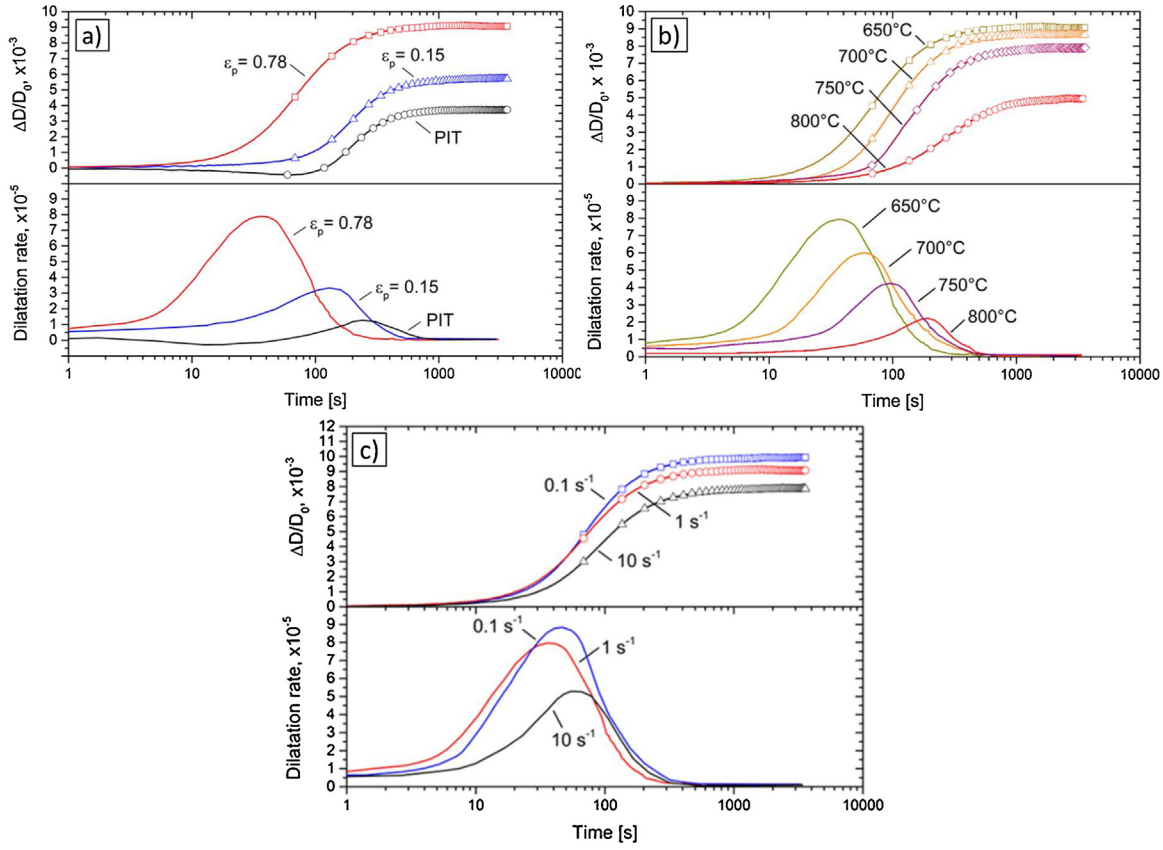

Fig. 5 – Relative dilation and dilatation rate curves gathered during the isothermal tempering of specimens (a) treated with and without ausforming, (b) ausformed at various temperatures and (c) ausformed at various strain rates in comparison.

transformation stage. The amount of defects increased with increasing ausforming strain. More nucleation sites implied that more austenite could be decomposed into bainite with a higher rate. The ausforming also contributed to mechanical stabilization of deformed austenite through accumulated strain and dislocations. As a result, mechanical driving force of nucleation sites became higher which was advantageous for the isothermal bainitic phase transformation, in which the total driving force required for diffusionless growth was raised [29,30]. On the other hand, retardation of the bainitic transformation because of increased ausforming temperature is presented for the examined steel in Fig. 5**b**. At high ausforming temperatures such as 800 °C, strain-induced dislocations were compensated by effect of dynamic and static recovery, in which the mechanical driving force was necessarily reduced [38]. Consequently, the total driving force for diffusionless growth was decreased, because distortion energy inherited from deformation to transformation stage was lowered. According to Zou et al. [37], reduction of driving force led to a delay of incubation time and thus decrease in the amount of bainite.

Fig. 5**c** depicts the influences of strain rate on the kinetics of bainitic transformation of investigated steel. In this work, it was found that the transformation rate was accelerated

when lower ausforming strain rate was applied. It implied that increasing deformation rate generally led to a decrease in the amount of transformed bainite. The highest amount of transformed bainite was obtained at the strain rate of $0.1\,s^{-1}$. The result was inconsistent to the fact that higher strain rate increased both dislocation densities in prior austenite and nucleation sites for the bainitic transformation, which subsequently led to an acceleration of transformation kinetics. Chen et al. [29,40] performed experiments to examine effects of strain rate during ausforming on the kinetics of bainite transformation. It was though reported that such relation most likely occurred in some medium/low carbon steels, in which the ausforming caused the inconsistent mechanism of dislocation rearrangement.

3.4. *Microstructure characteristics*

Microstructure of the PIT specimens and specimens heat-treated and ausformed at 650 °C with the strain rate of $1\,s^{-1}$ up to the final strain of 0.78 were characterized by LOM and SEM, as demonstrated in Fig. 6. According to the used processing routes, three phases could form in the investigated steel, namely, BF, RA in thin film and/or block form and M/A constituent [39,40]. The presence of M/A constituent verified that the bainite transformation was incomplete. The amount of occurred martensite was consistent with the dilatation curves of the last cooling stage of the heat treatment with ausforming. By means of the color etching with Klemm's solution, in the LOM micrographs of specimens BF and martensite appeared as bright and dark brown areas, respectively, while RA was white zones [41], as illustrated in Fig. 6**a** and **d**. The microstructures of PIT specimens showed a formation of highly elongated BF, RA, and martensitic structures, whereas those of specimens heat-treated with ausforming were obviously refined with reduced amount of martensite. This was due to that the movement of dislocations caused by ausforming increased the boundary areas of austenitic grain per unit volume and thus led to the refinement of BF and RA structures at the end of heat treatment [22,32]. Furthermore, SEM micrographs in Fig. 6**b** and **e** exhibited well the effect of ausforming on the microstructure refinement. It is obvious that the ausforming completely altered the microstructure of steel by replacing large blocks and elongated film-like areas with many tiny heterogeneous blocks and film-like morphologies. Observed microstructures at higher magnitude are depicted in Fig. 6**c** and **f**. Hereby, the difference between RA and M/A constituent could be distinguished by their appearances. The RA phase was characterized in the form of either white thin-films located within sheaf-shape matrix of BF or island blocks with bright mellow appearance surrounded by matrix of granular BF. The M/A constituent was recognized as a mixture constituent, which consisted of martensite with rough appearance embedded within thin boundaries of RA, as shown with the red polygons in Fig. 6**c** and **f**. The resulted microstructures of ausformed specimens were finer and more uniformly distributed. Though undesired M/A constituent could be considerably reduced by ausforming, the morphological distribution needed to be further controlled properly, since this may also affect the deterioration of ductility of steel [32]. Likewise, the amount of defects significantly depended on ausforming strain. Increasing the strain led to an increase in dislocation densities and splitting prior austenitic grains into several small sub-grain structures. Hereby, in the individual RA subsections, the area of growth was restricted and the ratio of carbon concentration per unit volume was increased that finally resulted in enhanced stability [7]. Furthermore, the variation of temperature and strain rate of ausforming also played an essential role in microstructure refinement due to static and dynamic recovery occurred [38,42]. When the temperature and/or strain rate of ausforming was increased, deformation induced dislocations partially vanished and the increase of sub-grains became more difficult. Hereby, the potential of grain refinement was greatly reduced and thus

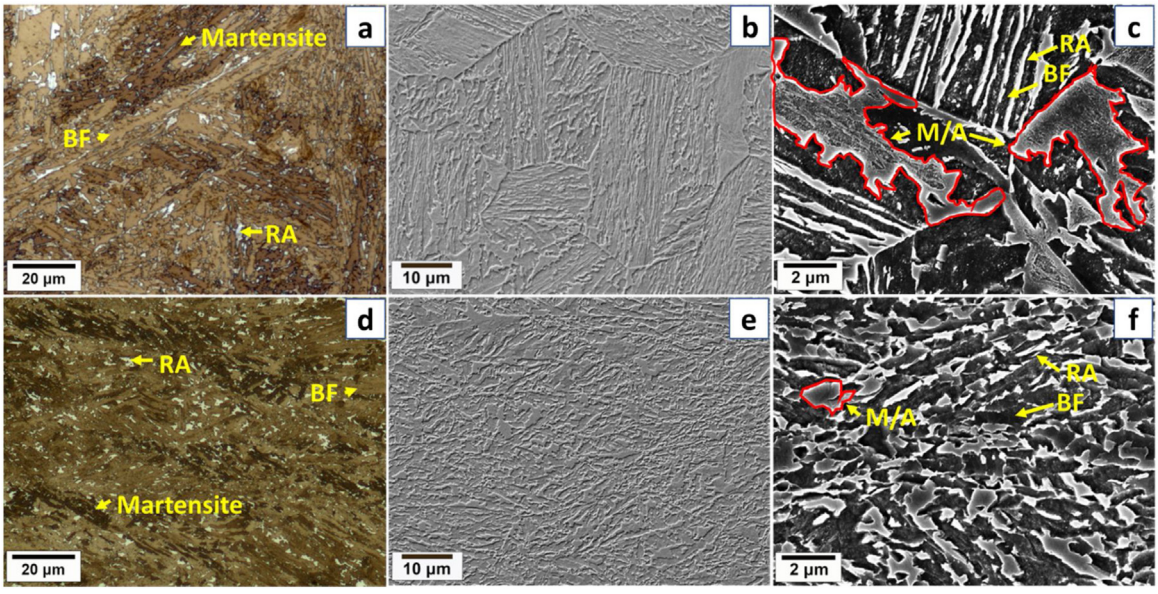

Fig. 6 – Observed microstructures of specimens subjected to PIT (a)–(c) and ausforming (d)–(f) at 650 °C under the strain rate of $1\,s^{-1}$ up to the strain of 0.78 and followed by isothermal tempering at 400 °C for 1 h.

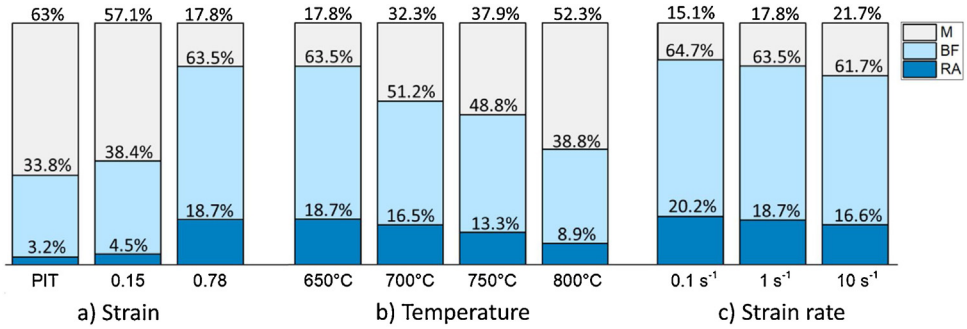

Fig. 7 – Phase fractions of treated steels determined by a combination of XRD measurements (RA fraction) and image analysis using an adaptive threshold (BF). M, BF and RA stands for martensite, bainitic ferrite and retained austenite, respectively. (Details of combination of temperature, strain, strain rate are found in Table 1).

Table 2 – Determined phase fractions of RA, BF and martensite by XRD and LOM. (Details of combination of temperature, strain, strain rate are found in Table 1).

Ausforming parameter	Deformation condition	RA_{XRD}	BF_{LOM}	M_{CAL}
Strain	PIT	3.2 ± 1.4	33.8 ± 3.9	63.0
	0.15	4.5 ± 0.9	38.4 ± 6.2	57.1
	0.78	18.7 ± 1.3	63.5 ± 5.6	17.8
Temperature (°C)	650	18.7 ± 1.3	63.5 ± 5.6	17.8
	700	16.5 ± 1.2	51.2 ± 6.5	32.3
	750	13.3 ± 1.5	48.8 ± 4.6	37.9
	800	8.9 ± 1.7	38.8 ± 4.9	52.3
Strain rate (s^{-1})	0.1	20.2 ± 1.5	64.7 ± 6.1	15.1
	1	18.7 ± 1.3	63.5 ± 5.6	17.8
	10	16.6 ± 1.2	61.7 ± 6.4	21.7

led to a formation of blocky RA and M/A constituent instead of film-like RA.

3.5. *Phase fraction analysis*

The XRD patterns of specimens undergoing various ausforming conditions were analyzed. The low relative intensity peaks of (111), (200), (220) and (311) planes, which took place at a diffraction angle of 43°, 48°, 74°, and 91° were corresponding with the diffraction planes of FCC RA, while the other peaks concerned either BCC bainite or martensite. Note that for multiphase steels, it was relatively difficult to distinguish the pattern of the martensitic and bainitic phases, because both exhibited BCC pattern [43]. Thus, the XRD patterns obtained from the investigated steels in this work were classified into the BCC-BF and/or martensite with FCC-RA. The amount of RA was hereby calculated by means of the Rietveld refinement method incorporated with the XRD patterns. On the other hand, the area fraction of BF was estimated from OM micrographs by an adaptive threshold method. Finally, phase fractions of martensite could be then calculated with the assumption that only three constituents, namely, RA, BF and martensite were formed in all ausformed specimens. As shown, in Fig. 7 along with more details in Table 2, the phase fractions of RA and BF increased and that of martensite decreased with increasing the ausforming strain. On the other hand, increasing the ausforming temperature and strain rate noticeably caused the reductions of RA and BF phase fractions while larger amount of martensite. This was due to grain refinement mechanism induced by ausforming, which contributed to mechanical stabilization of austenite by segmenting its grains into small sub-grains. Such enhanced austenite stability hindered the martensitic transformation. Moreover, the increase of BF phase fraction was likely because of acceleration of bainitic transformation affected by the mechanical driving force. It is noted that optimum phase fractions of examined steel would be 20% of RA, 65% of BF and 15% of martensite that were observed in the specimen deformed at the temperature, strain and strain rate of 650 °C, 0.78 and 0.1 s^{-1}, respectively. Additionally, rather high phase fraction of martensite of 63% was found in the PIT specimens due to the instability of austenite and somewhat lower formation rate of bainite.

3.6. *Hardness*

The macro-Vickers hardness values measured on the entire cross-sectional surface of all investigated specimens are provided in Fig. 8. It is seen that ausforming temperature, strain and strain rate considerably affected the hardness and thus strength of ausformed steel. The hardness decreased by increasing the ausforming strain, whereas it increased when the deformation temperature and strain rate became higher. These overall results agreed well with the ratio and individual hardness of all identified constituents in the thermo-mechanically treated specimens [44]. An increased martensitic phase fraction led to a higher hardness of specimens, while a reduction of hardness was caused by larger

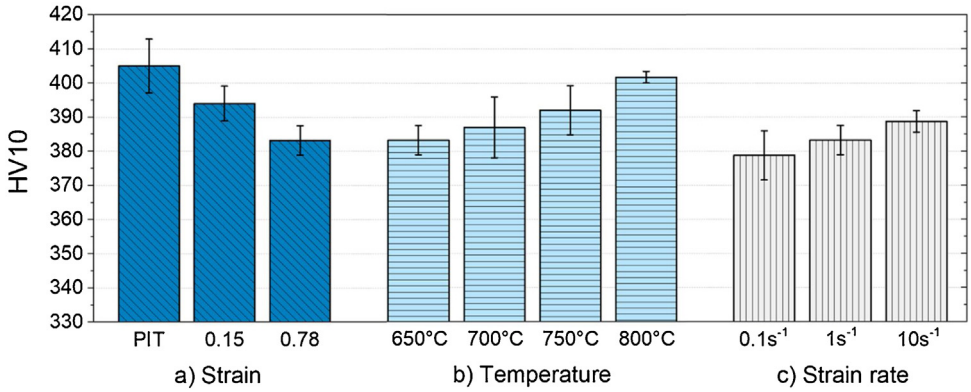

Fig. 8 – Vickers hardness values as a function of different ausforming parameters: a) strain, b) temperature and c) strain rate. (Details of combination of temperature, strain, strain rate are found in Table 1).

phase fraction of RA. The highest hardness of about 405 HV was obtained from the PIT specimens, which exhibited larger amount of martensite of 63% and a few RA of 3%. Nevertheless, the specimens deformed at 650 °C with strain and strain rate of 0.78 and 0.1 s^{-1}, respectively showed a relatively low hardness, in which 15% of martensite and 20% of RA were observed.

4. Conclusions

The present study aimed to investigate the influences of ausforming temperature, strain and strain rate on the kinetics of isothermal transformation, microstructure characteristics and hardness of a low-carbon carbide-free bainitic steel. The conclusions can be drawn as follows:

- The applied ausforming accelerated the transformation kinetics and thus increased phase fraction of bainite in steel. This was due to the impact of mechanical driving forces on the decomposition of austenite.
- Ausforming temperature, strain and strain rate greatly affected both magnitude of defects and austenite grain size of steel. Its bainitic transformation kinetics was directly governed by the heterogeneous nucleation sites and stability of austenite.
- The ausforming refined the prior austenitic grains and increased the matrix strength. As a result, retained austenite was stabilized and thus led to lowered fractions of martensite.
- The final hardness of steel was defined by the martensitic phase fraction which depended on all ausforming parameters. The correlation between microstructure features and other mechanical properties will be further studied.

Data availability

The raw/processed data required to reproduce these findings cannot be shared at this time as the data also forms part of an ongoing study.

Conflicts of interest

The authors declare no conflicts of interest.

Acknowledgments

We wish to thank The National Science and Technology Development Agency (NSTDA) of Thailand for facilitating XRD measurement and remunerative references data, Marc Ackermann, Michael Schillheim, and technician staffs at IEHK for the extraordinary technical assistances.

REFERENCES

[1] Barbacki A. The role of bainite in shaping mechanical properties of steels. J Mater Process Technol 1995;53(1):57–63.
[2] Cornide J, Garcia-Mateo C, Capdevila C, Caballero FG. An assessment of the contributing factors to the nanoscale structural refinement of advanced bainitic steels. J Alloys Compd 2013;577:S43–7.
[3] Garcia-Mateo C, Caballero FG, Bhadeshia HKDH. Acceleration of low-temperature bainite. Isij Int 2003;43(11):1821–5.
[4] Caballero FG, Garcia-Mateo C. The processing of nanocrystalline steels by solid reaction. In: Whang Sung H, editor. Nanostructured metals and alloys: processing, microstructure, mechanical properties and applications. Woodhead Publishing; 2011. p. 85–117.
[5] Liu W, Zhang B, Zhao A, Guo H, Sun S. Control of morphology and dimension of blocky retained austenite in medium-carbon steel. Mater Res Express 2019;6(1):016526.
[6] Bhadeshia HKDH, Edmonds DV. Bainite in silicon steels: new composition–property approach Part 1. Met Sci J 1983;17(9):411–9.
[7] Bhadeshia HKDH. Bainite in steels: transformations, microstructure and properties. 2nd ed. London IOM Communications; 2001.
[8] Wang SC, Yang JR. Effects of chemical composition, rolling and cooling conditions on the amount of martensite/austenite (M/A) constituent formation in low carbon bainitic steels. Mater Sci Eng A 1992;154(1):43–9.
[9] Lian J, Yang H, Vajragupta N, Münstermann S, Bleck W. A method to quantitatively upscale the damage initiation of

dual-phase steels under various stress states from microscale to macroscale. Comput Mater Sci 2014;94:245–57.
[10] Liu W, Liang J, Jiang Y, Zhang B, Zhao A. A study of blocky retained austenite and properties under variously heat-treated ultra-fine bainitic steel. Mater Res Express 2019;6(10):105607.
[11] Shimanov M, Korpala G, Terzic A, Kawalla R. Bainitic steels: their characteristics and applications. Key Eng Mater 2016;684:104–10.
[12] Matsuda H, Bhadeshia HKDH. Kinetics of the bainite transformation. Proceedings of the royal society a: mathematical. Phys Eng Sci 2004;460(2046):1707–22.
[13] Yang HS, Bhadeshia HKDH. Designing low carbon, low temperature bainite. Mater Sci Technol 2008;24(3):335–42.
[14] Ravi AM, Sietsma J, Santofimia MJ. Exploring bainite formation kinetics distinguishing grain-boundary and autocatalytic nucleation in high and low-Si steels. Acta Mater 2016;105:155–64.
[15] Takahashi M. Recent progress: kinetics of the bainite transformation in steels. Curr Opin Solid State Mater Sci 2004;8(3–4):213–7.
[16] Bhadeshia HKDH. Nanostructured bainite. Proceedings of the royal society a: mathematical. Phys Eng Sci 2010;466(2113):3–18.
[17] Li S, Zhu R, Karaman I, Arróyave R. Development of a kinetic model for bainitic isothermal transformation in transformation-induced plasticity steels. Acta Mater 2013;61(8):2884–94.
[18] Jiang H, Wu H, Tang D, Liu Q. Influence of isothermal bainitic processing on the mechanical properties and microstructure characterization of TRIP steel. J Univ Sci Technol Beijing Miner Metall Mater 2008;15(5):574–9.
[19] Saha-Podder A, Bhadeshia HKDH. Thermal stability of austenite retained in bainitic steels. Mater Sci Eng A 2010;527(7–8):2121–8.
[20] Shipway PH, Bhadeshia HKDH. Mechanical stabilisation of bainite. Mater Sci Technol 1995;11(11):1116–28.
[21] Yang JR, Huang CY, Hsieh WH, Chiou CS. Mechanical stabilisation for bainitic reaction in a Fe-Mn-Si-C bainitic steel. Le Journal de Physique IV 1995;05-(C8):497–502.
[22] Zhao L, Qian L, Zhou Q, Li D, Wang T, Jia Z, et al. The combining effects of ausforming and below-Ms or above-Ms austempering on the transformation kinetics, microstructure and mechanical properties of low-carbon bainitic steel. Mater Des 2019;183:108123.
[23] Meng JY, Zhao LJ, Huang F, Zhang FC, Qian LH. Isothermal transformation, microstructure and mechanical properties of ausformed low-carbon carbide-free bainitic steel. Mater Sci Forum 2018;941:329–33.
[24] Yang HS, Bhadeshia HKDH. Austenite grain size and the martensite-start temperature. Scr Mater 2009;60(7):493–5.
[25] Zhao J, Jia X, Guo K, Jia NN, Wang YF, Wang YH, et al. Transformation behavior and microstructure feature of large strain ausformed low-temperature bainite in a medium C-Si rich alloy steel. Mater Sci Eng A 2017;682:527–34.
[26] Golchin S, Avishan B, Yazdani S. Effect of 10% ausforming on impact toughness of nano bainite austempered at 300 °C. Mater Sci Eng A 2016;656:94–101.
[27] Gong W, Tomota Y, Adachi Y, Paradowska AM, Kelleher JF, Zhang SY. Effects of ausforming temperature on bainite transformation, microstructure and variant selection in nanobainite steel. Acta Mater 2013;61(11):4142–54.
[28] Chen G, Xu G, Hu H, Yuan Q, Zhang Q. Effect of strain rate on deformation resistance during ausforming in Fe-C-Mn-Si high-strength bainite steels. Steel Res Int 2018;89(11):1800201.
[29] Singh SB, Bhadeshia HKDH. Quantitative evidence for mechanical stabilization of bainite. Mater Sci Technol 1996;12(7):610–2.
[30] He BB, Xu W, Huang MX. Effect of ausforming temperature and strain on the bainitic transformation kinetics of a low carbon boron steel. Philos Mag 2015;95(11):1150–63.
[31] Wirths V. Prozessführung und zyklisches Werkstoffverhalten von karbidfreien bainitischen Stählen [Doctoral thesis]. Aachen: Rheinisch-Westfällischen Technischen Hochschule Aachen; 2016.
[32] Zhao L, Qian L, Liu S, Zhou Q, Meng J, Zheng C, et al. Producing superfine low-carbon bainitic structure through a new combined thermo-mechanical process. J Alloys Compd 2016;685:300–13.
[33] Ferraris SA, Danón CA. Desdoblamiento de la transformación martensítica en un acero F82H de activación neutrónica reducida. Matéria (Rio J.) 2018;23(2):1–10.
[34] Tao X, Han L, Gu J. Splitting phenomenon in martensitic transformation of X12CrMoWVNbN10-1-1 steel. Int J Mater Res 2015;105(6):565–71.
[35] Gui X, Gao G, Guo H, Zhao F, Tan Z, Bai B. Effect of bainitic transformation during BQ&P process on the mechanical properties in an ultrahigh strength Mn-Si-Cr-C steel. Mater Sci Eng A 2017;684:598–605.
[36] Tian J, Xu G, Jiang Z, Wan X, Hu H, Yuan Q. Transformation behavior and properties of carbide-free bainite steels with different Si contents. Steel Res Int 2019;90(3):1800474.
[37] Zou H, Hu H, Xu G, Xiong Z, Dai F. Combined effects of deformation and undercooling on isothermal bainitic transformation in an Fe-C-Mn-Si alloy. Metals 2019;9(2):138.
[38] Hu H, Xu G, Dai F, Tian J, Chen G. Critical ausforming temperature to promote isothermal bainitic transformation in prior-deformed austenite. Mater Sci Technol 2019;35(4):420–8.
[39] Guo H, Feng X, Zhao A, Li Q, Chai M. Effects of ausforming temperature on bainite transformation kinetics, microstructures and mechanical properties in ultra-fine bainitic steel. J Mater Res Technol 2019;9(2):1151.
[40] Fan HL, Zhao AM, Li QC, Guo HH, He JG. Effects of ausforming strain on bainite transformation in nanostructured bainite steel. Int J Miner Metall Mater 2017;24(3):264–70.
[41] Kučerová L, Opatová K, Jandová A. Microscopy and imaging science: Practical approaches to applied research and education. In: Méndez-Vilas A, editor. Metallography of AHSS steels with retained austenite. Badajoz, Spain: Formatex Research Center; 2016. p. 455–63.
[42] Seshacharyulu T, Dutta B. Influence of prior deformation rate on the mechanism of b -& a+b transformation in Ti–6Al–4V. Scr Mater 2002;46:673–8.
[43] Talebi S, Ghasemi-Nanesa H, Jahazi M, Melkonyan H. In situ study of phase transformations during non-isothermal tempering of bainitic and martensitic microstructures. Metals 2017;7(9), 346(1–13).
[44] Wang X, Zurob HS, Xu G, Ye Q, Bouaziz O, Embury D. Influence of microstructural length scale on the strength and annealing behavior of pearlite, bainite, and martensite. Metall Mater Trans A 2013;44(3):1454–61.